

出國報告（出國類別：國際會議）

## 赴美國夏威夷參加 2018 年亞洲大洋洲 地球科學聯合研討會

服務機關：中央氣象局地震測報中心

姓名職稱：陳燕玲課長、羅翊菁技佐及賴姿心技佐

派赴國家/地區：美國夏威夷

出國期間：107 年 5 月 30 日至 107 年 6 月 14 日

報告日期：107 年 6 月 27 日

# 摘 要

亞洲大洋洲地球科學聯合研討會(Asia Oceania Geosciences Society, AOGS) 是亞洲地區規模最大之地球科學研究與應用的國際聯合研討會，此會議每年廣邀各國從事地球科學相關研究之學者，提供大家發表研究成果與互相交流的機會。

為分享本局在地震測報工作之成果，本局指派地震測報中心陳燕玲課長、羅翊菁及賴姿心 2 位技佐前往美國夏威夷參加本年度會議。陳員等 3 人於會議中以海報形式發表其個人之研究論文，論文題目分別為「A Study on the Correlation of the Stress and Earthquake Frequency-Magnitude Distribution b Value in Taiwan」、  
「Modeling Regional Waveforms from Explosion Source with Realistic Surface Topography」及「Determination of a local magnitude scale using earthquake data recorded by the borehole seismic network in Taiwan」，透過與會發表研究成果，就近與各國專家學者進行實質交流及觀摩，除對本局地震測報業務之發展有所助益外，亦可提升陳員等 3 人之學術研究創新及精進能力。

# 目 次

一、目的	1
二、過程	2
三、心得與建議	15
四、附錄	16

# 一、目的

亞洲大洋洲地球科學聯合研討會(Asia Oceania Geosciences Society, AOGS)於每年夏季於亞太地區的國家輪流主辦，匯集來自世界各地關心亞太地區地球科學各個領域的學者及研究生一同參與，目的是希望能夠透由交流和討論的機會，能展現各自的研究成果，激盪出更多的火花，以解決學術界、研究機構和公眾中重要的地球科學問題，讓交流的成果在研究上得以幫助。

今年(2018)訂於 6 月 3 日至 6 月 8 日於夏威夷盛大舉行，為分享我國在地震測報工作之研發成果與觀摩各國相關之技術及經驗，本局指派地震測報中心陳燕玲課長、羅翊菁及賴姿心技佐 3 人參加透過人發表個人論文成果海報及參與最佳優秀學生論文比賽，除可展現陳員 3 人平時工作的研究成果，並與來自世界各地的專家學者在研究上交換想法與建議，不僅可促進本局地震測報作業與各國地震領域之交流，亦可提升陳員 3 人學術研究創新及精進之能力。

## 二、過程

本年度會議主題涵蓋大氣科學(Atmospheric Sciences)、生物科技(Biogeosciences)、水文科學(Hydrological Sciences)、跨域地質學(Interdisciplinary Geosciences)、海洋科學(Ocean Sciences)、古海洋和古氣候學(Paleoceanography and Paleoclimatology)、行星科學(Planetary Sciences)、太陽與地球科學(Solar and Terrestrial Sciences)、固態地球科學(Solid Earth Sciences)及特別演講(Special Sessions)，研討會線上議程如下：

<http://www.asiaoceania.org/aogs2018/public.asp?page=sessionList.htm>

，陳員 3 人主要參加固態地球科學議題之議程。

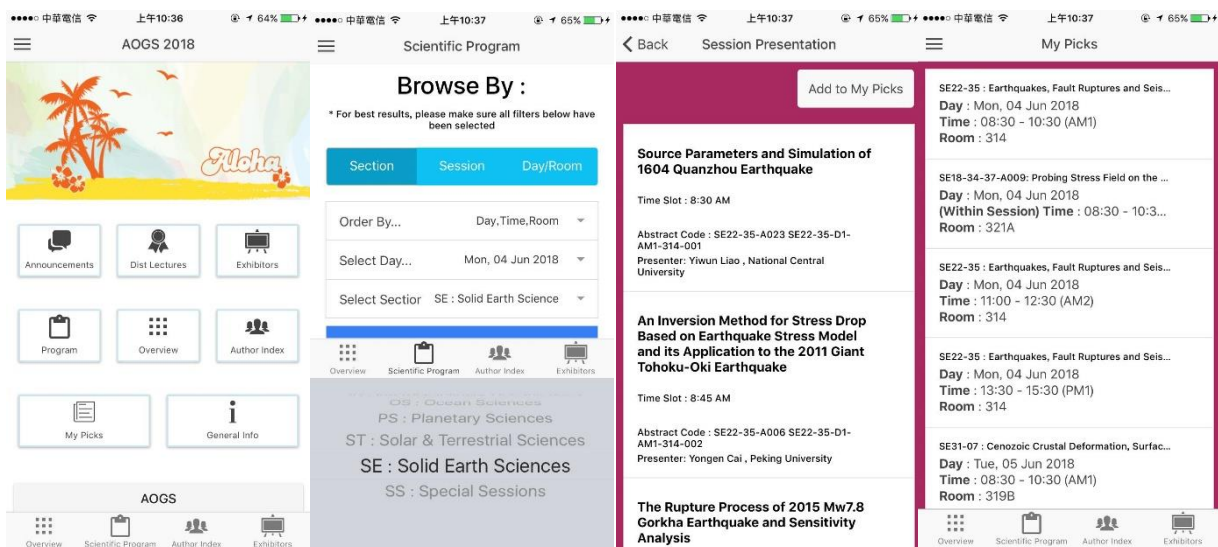
### (一)參訪行程

日期	工作摘要
107年5月30日(三)	赴夏威夷
107年5月31日(四)至 107年6月2日(六)	搭乘華航CI2班機，21時10分起飛出發前往夏威夷，於當地時間5月30日12時45分抵達檀香山國際機場。由於航班限制，因此提早出發，除可提早熟悉會場附近場域，並調整時差及安頓各自作息以養精蓄銳參加會議。
107年6月3日(日)	準備海報報告內容及提早去會場報到領取識別證。
107年6月4日(一)	參與地震、斷層破裂及地震學等相關研究議題與海報。 中午參加地震斷層破裂及地震學議題午餐(session lunch)。 晚上參加大會reception活動。
107年6月5日(二)	參與動態模型與機制、地震斷層破裂及地震學、利用數據解析地球與地震模擬等相關研究議題與海報。
107年6月6日(三)	參與地震斷層破裂及地震學、利用數據解析地球與地震模擬等相關研究議題與海報。
107年6月7日(四)	準備海報並發表個人海報、羅員及賴員參與最佳優秀學生論文比賽。
107年6月8日(五)	參與地球與地震模擬等相關研究議題與海報。

107年6月9日(六)至 107年6月13日(三)	陳員於會議結束後6月10日(日)返臺，搭乘華航CI1班機，14時55分起飛，於臺灣時間6月11日19時30分抵達桃園國際機場。  羅員與賴員欲體驗夏威夷火山行程，故於6月13日(三)返臺，搭乘華航CI1班機，14時55分起飛，於臺灣時間6月14日19時30分抵達桃園國際機場。
107年6月14日(四)	返回臺北

## (二)參與有關固態地球科學(Solid Earth Science)議題的議程

近幾年各大研討會為節能減碳提倡無紙化後，以往非常厚重的紙本議程，現今都由電子 app 取代，可方便掌握議程資訊，app 介面如下圖，選取好欲聆聽的議題後，可以加入「我的選擇(my picks)」，最後會有 1 份專屬你自己的「行程(schedule)」。



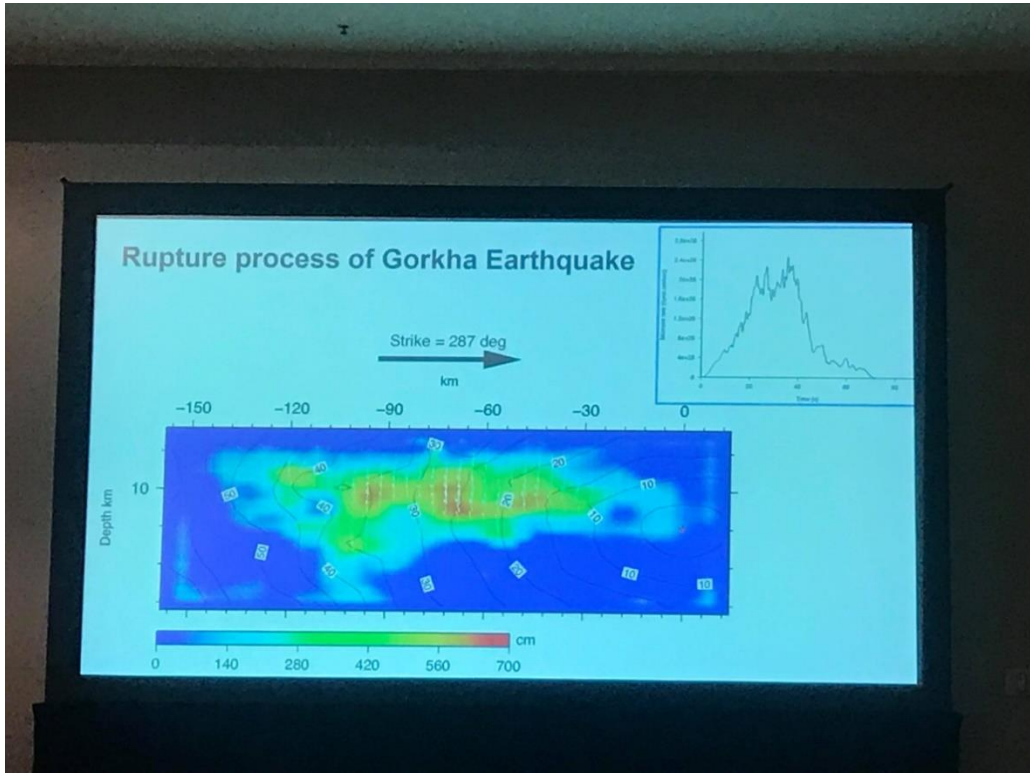
圖一、(左至右)分別為 app 主頁面、選取議程、議程內容及「我的選擇(my picks)」。



圖二、各個會議室裡面都有精彩的議題。



圖三、有關臺灣淺層速度構造的議題，講者為國震中心林哲民研究員。



圖四、與廓爾喀(Gorkha)地震有關之議題。



圖五、有關 PSHA 之議題，講者為新加坡南陽理工大學詹忠翰研究員。





圖六、有關噪聲(ambient noise)之議題，講者為猶他大學林凡奇。

### (三)本局參與人員發表研究成果

#### 1. 陳燕玲課長

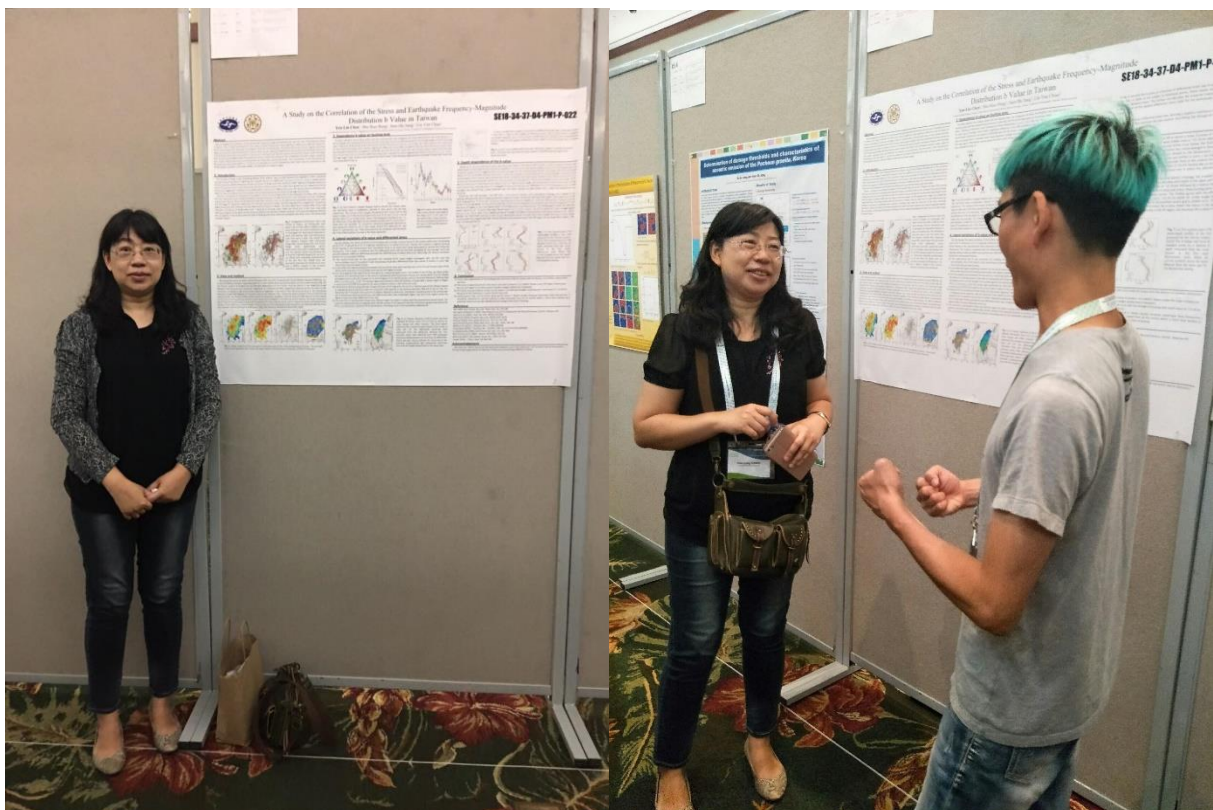
陳員發表論文的題目為「A Study on the Correlation of the Stress and Earthquake Frequency-Magnitude Distribution b Value in Taiwan」，中文題目為「臺灣地區應力與地震頻率規模分布及地震b值的相關性研究」。

上述研究使用本局地震觀測網地震目錄的343,581地震與2,640個地震震源機制解，用以描繪臺灣地震頻率規模分布與地震b值之空間變化，研究其與斷層錯動類型與地殼應力型態的相關性。地震b值的估計結果顯示，在95%的信賴區間內，各類震源機制的地震b值顯然存在著明顯的差異，逆斷層b值最低( $0.82 \pm 0.02$ )，走向滑移斷層b值居於中間( $0.89 \pm 0.03$ )，正斷層b值最高( $1.03 \pm 0.09$ )，所得結果與全球和其他區域得到相當一致的地震觀察結果。

估算臺灣3種震源機制型態的地震b值結果顯示，具有非常顯著的差異，其中逆斷層錯動型態的震源機制具有最低的地震b值，走向滑移斷層錯動型態具有中間值，正斷層

錯動型態具有最高的地震b值，這個結果與全球性或區域性地震活動的相關研究都有很好的一致性。在地震b值的側向分布研究顯示，其與主要的斷層錯動機制、地殼變形及應力型態都有非常良好的相關性。臺灣在強大的東西向縮短與差異應力作用下，造成在東臺灣和西臺灣的兩個南北走向的逆衝斷層帶，其具有較低的地震b值；在中臺灣狹長南北向的山脈內或山脈間，受到較小的拉張應力作用，主要受到走向滑移和正斷層作用，其具有較高的地震b值。在地震b值的深度分布研究顯示，地震b值隨深度單調遞減至大約於15-20公里深度終止，顯示地震b值與應力呈現反比關係，並且證實在臺灣造山帶底下具有弱質中部地殼，並存在一層脆塑性的轉變帶。

簡言之，本研究首先驗證在臺灣造山帶之地震b值與斷層錯動型態及地殼應力同樣具有通用的對應相關。區域地震b值的變化與地殼變形及應力架構的良好相關性，充分顯現了區域的震源構造特性。隨震源深度變化的地震b值顯示，臺灣底下的弱質中部地殼，在約15-20公里深度，存在一層脆塑性的轉換帶。



圖七、陳員與海報合影。

# A Study on the Correlation of the Stress and Earthquake Frequency-Magnitude Distribution b Value in Taiwan

Yen-Lin Chen<sup>1</sup>, Shu-Huei Hung<sup>2</sup>, Juen-Shi Jiang<sup>1</sup>, Lin-Yun Chiao<sup>3</sup>

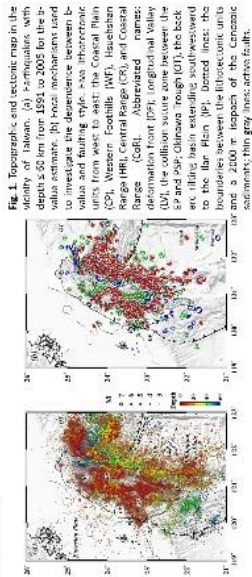
<sup>1</sup> Center for Weather, Taiwan, <sup>2</sup> Department of Geosciences, National Tsing-Tung University, Taiwan, <sup>3</sup> Institute of Oceanography, National Tsing-Tung University, Taiwan

## Abstract

We investigate the correlation of the earthquake frequency-magnitude distribution with the type of faulting and stress in Taiwan. The b values are categorized for three types of focal mechanisms: strike-slip, normal, and thrust. The lateral distribution of b values shows a good correlation with the predominant faulting mechanism, crustal deformation, and stress patterns. The two MS striking thrust zones in western and eastern Taiwan under the E-W shortening and differential stress yield the lowest b values than those in the In-between mountain ranges along the Taiwan orogenic belt, dominated by strike-slip and normal faults. The transition of the macroseismicity from the In-between mountain ranges to the Coastal Plain is associated with the In-between mountain range.

## 1. Introduction

The b value or slope in the Gutenberg-Richter (G-R) relation,  $\log_{10} N = a - bM$ , between the logarithm of the cumulative number  $N$  of earthquakes of magnitude  $M$  or greater versus the magnitude (Coulter & Richter, 1945), is widely used to characterize the relative frequency of the occurrence of large and small events for both regional and global seismicity. Since Schorlemmer et al. (2005) found the decrease of b value in the order from public normal, strike-slip to thrust zones and suggest a universal inverse dependence of b value on differential stress, this spatiotemporal variation of b value has been used as a stress indicator (e.g., Wang & Chen, 2009; Wang et al., 2010; Wang et al., 2011; Wang et al., 2012; Wang et al., 2013; Wang et al., 2014; Wang et al., 2015; Wang et al., 2016; Wang et al., 2017; Wang et al., 2018; Wang et al., 2019; Wang et al., 2020; Wang et al., 2021; Wang et al., 2022; Wang et al., 2023; Wang et al., 2024; Wang et al., 2025). The two subduction zones of opposite polarity along the Ryukyu and Okinawa Trench to the northeast and south of Taiwan respectively (Fig. 1a). Since the late Miocene when the northern Luzon arc formed by the tectonically-subducting EP under the IOP began to obliquely collide onto the Chinese continental margin, the still ongoing active orogenic has created the high-relief orogenic belts and structures in Taiwan. The very rapid rate of crustal deformation and frequent occurrence of earthquakes with a diversity of faulting styles make the island one of the most seismically hazardous regions in the world. In this study, we examine the lateral and depth variations of b value and compare whether the b value with the type of faulting and stress observed worldwide and localities in the tectonically active Taiwan.



## 2. Data and method

We choose the events at depth < 60 km between 1973 and 2015 located by the Central Weather Bureau (CWB) (Fig. 1a). A total of 2640 events with magnitude down to 2.0 and reliable focal mechanisms from our first-motion analysis (Fig. 1b) are further used to investigate the faulting style dependence of the b-value. Only the events in the magnitude range between the minimum and maximum magnitude of completeness (M<sub>C</sub>), respectively determined by the point of the maximum curvature in the incremental frequency-magnitude curve and of the stationarity drop in the cumulative frequency-magnitude curve, are used in this study. The minimum M<sub>C</sub> of the former nearly influenced by the detector capability of the local seismic stations has the lowest ( $\approx 1.5$ ) in the south-central and northern mountain areas and the highest ( $\approx 2.5$ ) offshore eastern Taiwan. The latter is related to the activity of the subaqueous zones which exceeds 6.0 in the collision zone since in southeast Taiwan and westward Ryukyu Trench offshore northeast Taiwan. The b-value and corresponding standard deviation are obtained with the linear least-squares method (Benjamin & Robinson, 1982; and maximum likelihood method (M<sub>L</sub>, 1982).

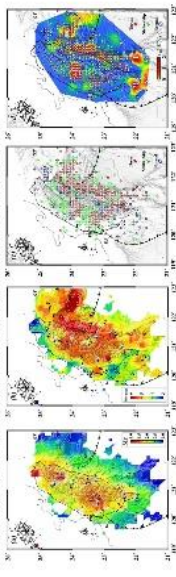


Fig. 2. Lateral variations of the minimum ( $M_C$ ) and maximum ( $M_C$ ) of the earthquake in Taiwan. The principal axes (a) and magnitude (b) of the main stress tensor based on minimum stress estimation of focal mechanisms.

## 3. Dependence b-value on faulting style

To extract whether the b-value varies with the faulting style, we extract the lateral and depth variations of b-value for three types of focal mechanisms with the compressive normal, strike-slip, and extensional normal faults, respectively. The b-value is categorized for three types of focal mechanisms: strike-slip, normal, and thrust. The lateral distribution of b values shows a good correlation with the predominant faulting mechanism, crustal deformation, and stress patterns. The two MS striking thrust zones in western and eastern Taiwan under the E-W shortening and differential stress yield the lowest b values than those in the In-between mountain ranges along the Taiwan orogenic belt, dominated by strike-slip and normal faults. The transition of the macroseismicity from the In-between mountain ranges to the Coastal Plain is associated with the In-between mountain range.

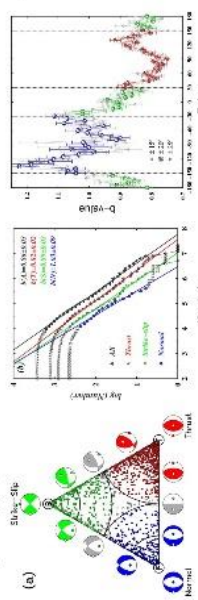


Fig. 3. (a) The triangular diagram used to classify the normal, strike-slip, and thrust types of focal mechanisms. The green, red, and blue colors represent the b-value for normal, strike-slip, and thrust faults, respectively. The b-value is categorized for three types of focal mechanisms: strike-slip, normal, and thrust. The lateral distribution of b values shows a good correlation with the predominant faulting mechanism, crustal deformation, and stress patterns. The two MS striking thrust zones in western and eastern Taiwan under the E-W shortening and differential stress yield the lowest b values than those in the In-between mountain ranges along the Taiwan orogenic belt, dominated by strike-slip and normal faults. The transition of the macroseismicity from the In-between mountain ranges to the Coastal Plain is associated with the In-between mountain range.

## 4. Lateral variations of b-value and differential stress

The lateral variations of b-value and maximum M<sub>C</sub> are compared with the stress field with such overlapping with the b-value. The b-value is categorized for three types of focal mechanisms: strike-slip, normal, and thrust. The lateral distribution of b values shows a good correlation with the predominant faulting mechanism, crustal deformation, and stress patterns. The two MS striking thrust zones in western and eastern Taiwan under the E-W shortening and differential stress yield the lowest b values than those in the In-between mountain ranges along the Taiwan orogenic belt, dominated by strike-slip and normal faults. The transition of the macroseismicity from the In-between mountain ranges to the Coastal Plain is associated with the In-between mountain range.

The lateral variations of b-value and maximum M<sub>C</sub> are compared with the stress field with such overlapping with the b-value. The b-value is categorized for three types of focal mechanisms: strike-slip, normal, and thrust. The lateral distribution of b values shows a good correlation with the predominant faulting mechanism, crustal deformation, and stress patterns. The two MS striking thrust zones in western and eastern Taiwan under the E-W shortening and differential stress yield the lowest b values than those in the In-between mountain ranges along the Taiwan orogenic belt, dominated by strike-slip and normal faults. The transition of the macroseismicity from the In-between mountain ranges to the Coastal Plain is associated with the In-between mountain range.

The lateral variations of b-value and maximum M<sub>C</sub> are compared with the stress field with such overlapping with the b-value. The b-value is categorized for three types of focal mechanisms: strike-slip, normal, and thrust. The lateral distribution of b values shows a good correlation with the predominant faulting mechanism, crustal deformation, and stress patterns. The two MS striking thrust zones in western and eastern Taiwan under the E-W shortening and differential stress yield the lowest b values than those in the In-between mountain ranges along the Taiwan orogenic belt, dominated by strike-slip and normal faults. The transition of the macroseismicity from the In-between mountain ranges to the Coastal Plain is associated with the In-between mountain range.

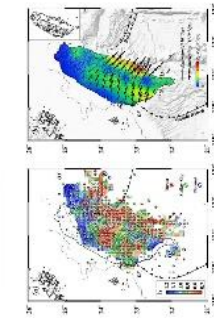


Fig. 4. Lateral variations of the minimum ( $M_C$ ) and maximum ( $M_C$ ) of the earthquake in Taiwan. The principal axes (a) and magnitude (b) of the main stress tensor based on minimum stress estimation of focal mechanisms.

## 圖八、陳員發表之海報內容。

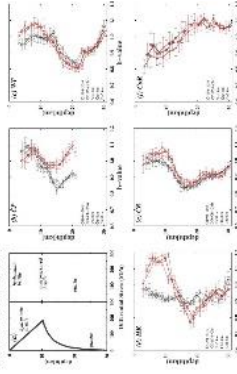
In Fig. 6, we plot the b-value as a function of differential strain rate in each grid shown in Fig. 5(d). In spite of the scatter of individual points, there clearly exists a negative correlation between them. This further corroborates the universal inverse dependence of the b-value on the applied differential stress holds for the tectonically very complex Taiwan.

Fig. 6. b-value versus differential strain rate, showing a negative correlation between them. The black line represents the best-fit curve, indicating the strength of the inverse relationship.

## 5. Depth dependence of the b-value

Klinger et al. (2001) used particle size distribution data to derive a linear increase of stress with depth down to brittle ductile transition at about 12 km and fairly weak middle crust at 25 km depth (Fig. 7a). However, Sogge (2002), suggested the constant strength for the overpressured brittle crust below the brittle-ductile transition of 3–3.5 km off-bounds in the western Taiwan thrust belt. To verify whether this crustal strength in Taiwan can be manifested by the b-values, we utilize their depth variations from the events divided by the lithological units at a number of overlapping depth intervals of constant width varying from 5 to 10 km and shifted in every 2 km (Figs. 7b-f). The error of the hypocentral depths from 10 to 15 km can be large, we exclude them in the analysis but include more events from 16 km to 20 km, to evaluate the potential influence of 100–300 m of depth uncertainty on the trend of the b-value. The b-value obtained with the same scaling and standard one in which the approach was removed.

Except for the Cok situated in the NW with a much thinner orogenic crust and distinct rheology, the b values in the settings affiliated with the Chinese continental margin all reveal a monotonic decrease with depth in the upper part of the crust ranging from ~5–20 to ~15–20 km, reaching the minima at depths of ~15–20 km followed by a reverse trend at further increasing depths. In conjunction with the inverse relation between b-value and stress, these turning points mark the peak strength in the crust below the brittle-ductile transition occurs. This finding agrees with the effective stress model proposed by Wang et al. (2002), and ~12 km depth weak peak strength recorded in neotectonic crust zones (Klinger et al., 2001). Besides, we notice that evolution of the CH-CH-atehahahh increased the b-value (lower the stress) in the upper crust between the orogenic belt (NW, HR and CR) and most prominently in the HR region, but decrease the b-value in the mid-crust beneath the CR.



## 6. Conclusion

The b-value dependence on the faulting style and stress holds for Taiwan with the diverse and complex deformation stresses and higher in the extensional mountain ranges (underlined In-between). The depth-varying b-value reveals a brittle upper crust with the strength increasing with depth down to ~15–20 km, followed by the transition to a weak, ductile mid-crust. Earthquakes in the vicinity of the same seismic zone in Taiwan usually comprise mixed-type focal mechanisms. It should be cautioned to use the reduced b-value estimated from all the points within a short time window as a preparation index. It can be also modified by the character of the state of faulting.

## Reference

Ali (1955). Bull. Earthq. Res. Inst. Tokyo Univ., 43, 235-239.  
Benjamin & Robinson (1982). Data Reduction and Error Analysis for the Physical Sciences, 2nd Ed., McGraw-Hill.  
Carena et al. (2001). J. Geophys. Res., 106, 993-1000.  
Chen et al. (2001). J. Geophys. Res., 106, 183-190.  
Chen et al. (2002). J. Geophys. Res., 107, 4185-4198.  
Chen et al. (2003). J. Geophys. Res., 108, 4100-4113.  
Chen et al. (2004). J. Geophys. Res., 109, 4100-4113.  
Chen et al. (2005). J. Geophys. Res., 110, 4100-4113.  
Chen et al. (2006). J. Geophys. Res., 111, 4100-4113.  
Chen et al. (2007). J. Geophys. Res., 112, 4100-4113.  
Chen et al. (2008). J. Geophys. Res., 113, 4100-4113.  
Chen et al. (2009). J. Geophys. Res., 114, 4100-4113.  
Chen et al. (2010). J. Geophys. Res., 115, 4100-4113.  
Chen et al. (2011). J. Geophys. Res., 116, 4100-4113.  
Chen et al. (2012). J. Geophys. Res., 117, 4100-4113.  
Chen et al. (2013). J. Geophys. Res., 118, 4100-4113.  
Chen et al. (2014). J. Geophys. Res., 119, 4100-4113.  
Chen et al. (2015). J. Geophys. Res., 120, 4100-4113.  
Chen et al. (2016). J. Geophys. Res., 121, 4100-4113.  
Chen et al. (2017). J. Geophys. Res., 122, 4100-4113.  
Chen et al. (2018). J. Geophys. Res., 123, 4100-4113.  
Chen et al. (2019). J. Geophys. Res., 124, 4100-4113.  
Chen et al. (2020). J. Geophys. Res., 125, 4100-4113.  
Chen et al. (2021). J. Geophys. Res., 126, 4100-4113.  
Chen et al. (2022). J. Geophys. Res., 127, 4100-4113.  
Chen et al. (2023). J. Geophys. Res., 128, 4100-4113.  
Chen et al. (2024). J. Geophys. Res., 129, 4100-4113.  
Chen et al. (2025). J. Geophys. Res., 130, 4100-4113.

## Acknowledgement

We thank the CWB for the earthquake database used in this study and Y.-C. Fial and H. Ke for discussions. This work was supported by the Ministry of Science and Technology (MOST) of Taiwan.

## 2. 羅翊菁技佐：

羅員發表論文的題目為「Modeling Regional Waveforms from Explosion Source with Realistic Surface Topography」，中文題目為「利用數值模擬的方法探討地表地形對於爆破源的影響」，該研究並參與本次會議學生優秀論文比賽。

上述研究係利用張偉(2012)等人的方法，在研究區域建模將曲面座標(Curvilinear Coordinate)轉成卡氏座標(Cartesian Coordinate)，再套入此研究區域之一維速度模型計算理論地震波形。由模擬結果可以明顯看到地表地形效應所帶來的誤差，因此地表地形在模擬中是不可忽略的。亦將模擬之波形經波速 8(公里/秒)平移過後隨著震央距排列，可以明顯看到 P 波及隨之而來的多重波相(multiple phase)，此多重波相是因為此區域速度變化梯度太大造成的三重行為(triplication)，因而產生出多重波相，本研究將利用此兩個波相的比值來判斷真實的震源深度，跟觀測資料比較厚的結果顯示，模擬之理論地震波所得的比值較接進的是深度在 800-100 公尺的震源深度。

最後，地震波模擬技術已是世界趨勢且在國外已經發展得很成熟，許多文章已經有利用數值模擬之理論地震波針對不同的地震參數討論，可提供觀測數據可靠的依據。共同與會之新加坡南洋理工大學的 Sehngji Wei 團隊前不久在 natural geoscience 發表了一篇利用 InSAR 針對北韓核試爆對此有更進一步的探討，羅員就近與 Sehngji Wei 討論了有關研究中位置及深度的限制，所獲之經驗對後續之研究將有很大的幫助。

# SE02-A050 Modeling Regional Waveforms from Explosion Source with Realistic Surface Topography

Yi-Ching Lo<sup>1,2</sup>, Li Zhao<sup>3</sup>, and Shu-Huei Hung<sup>1</sup>  
 1. Department of Geosciences, National Taiwan University, Taipei, Taiwan; 2. Central Weather Bureau, Taipei, Taiwan;  
 3. School of Earth and Space Sciences, Peking University, China.



## Summary

The Earth's surface topography has significant influence on the propagation of seismic waves, which in turn leads to complexities in recorded waveforms. In this study, we use finite difference method and strain Green tensor approach to investigate the effect of the surface topography near the source location on seismic waveforms. North Korea has conducted six nuclear tests since 2006, with the latest in September 2017 (Table 1.) The issue of nuclear explosions by North Korea are of great public concern and has attracted much seismological interests. Our goal is to examine the topography influence surrounding the nuclear explosion site as well as source-receiver geometry which can lead to significant effects on the recorded waveforms.

## Finite Difference Method

The finite-difference method (FDM, Zhang et al. 2012), which uses a conforming mesh to discretize the topography on the surface and interfaces (Figure 1), was adopted to compute the synthetics in local one-dimensional (1D) velocity model (Figure 2) with ETOPO1 topography (Figure 3).

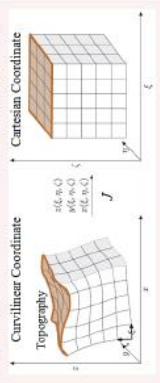


Figure 1. Schematic diagram for the curvilinear coordinate system (left) for the irregular mesh and the Cartesian coordinate system (right) for the regular mesh used by the finite-difference algorithm. Adapted from Zhang et al. (2012).

## Strain Green Tensor (SGT) Approach

We use the SGT approach (Zhao et al., 2006) to examine the effect on waveforms due to the uncertainty in source location and topography in the vicinity of the source. We save the SGTs in a small volume near the location of nuclear explosion given by the USGS, using a mesh with grid sizes of 200 m horizontally and 200 m vertically. The source-time function is a Gaussian, and the FDM waveforms are accurate up to ~1.5 Hz.

References  
 Zhang, W., Zhang Z., and Chen, X. (2012). Three-dimensional elastic wave numerical modeling in the presence of surface topography by a collocated-grid finite-difference method on curvilinear grid. *Geophysical Journal International*, 190, 133-178.  
 Zhao, L., Chen, P., and Jordan, T. H. (2006). Strain Green's tensors, reciprocity, and their applications to seismic source and structure analysis. *Bull. Seism. Soc. Am.*, 96, 1752-1783.

## Simulation Configuration

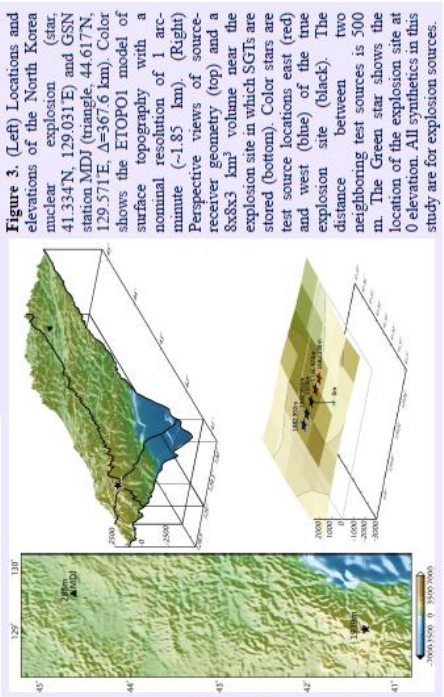


Figure 3. (Left) Locations and elevations of the North Korea nuclear explosion (star, 41.334°N, 129.031°E) and GSN station MDI (triangles, 44.617°N, 129.571°E, Δ=567.6 km). Color shows the ETOPO1 model of surface topography with a nominal resolution of 1 arc-minute (-1.85 km). (Right) Perspective views of source-receiver geometry (top) and a 8x8x3 km³ volume near the explosion site in which SGTs are stored (bottom). Color stars are test source locations east (red) and west (blue) of the true explosion site (black). The distance between two neighboring test sources is 500 m. The Green star shows the location of the explosion site at 0 elevation. All synthetics in this study are for explosion sources.

## Synthetic Seismograms with and without Topography

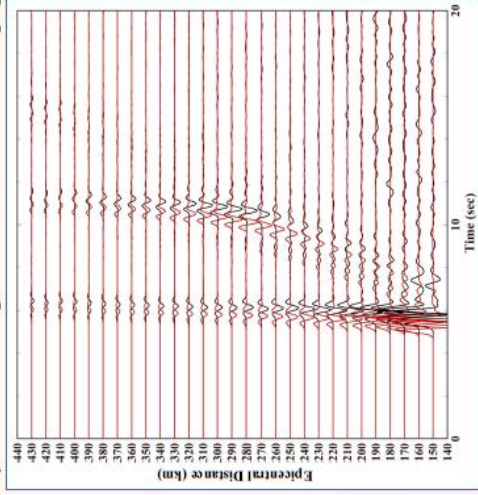


Figure 4. (Left) FDM synthetics around the P waves for a suite of epicentral distances from 150-430 km with (black) and without (red) topography. The source depth is 1 km. The waveforms are shifted in time with a wave speed of 8 km/s. Multiple arrivals can be seen following the first arriving P wave due to the velocity gradient in the 1D model (Figure 2). The topography-induced delay time and waveform distortion due to topography scattering can be seen in the black traces. The ratio between the maximum amplitudes of the first two arrivals is used to constrain the source depth (Figure 6).

## Comparison of Record and Synthetics

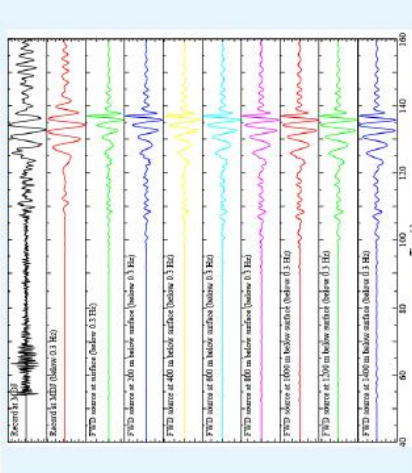


Figure 5. Comparison between synthetics computed with ETOPO1 topography and record at MDI. Traces from the top are: Unfiltered Z-component record obtained from Incorporated Research Institutions for Seismology (IRIS); low-pass filtered record with a cutoff frequency of 0.3 Hz; synthetics low-pass filtered in the same way from sources at the depths of 0 m, 200 m, 400 m, and 1000 m.

## Constraining Source Depth

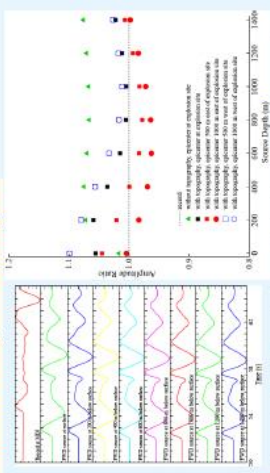
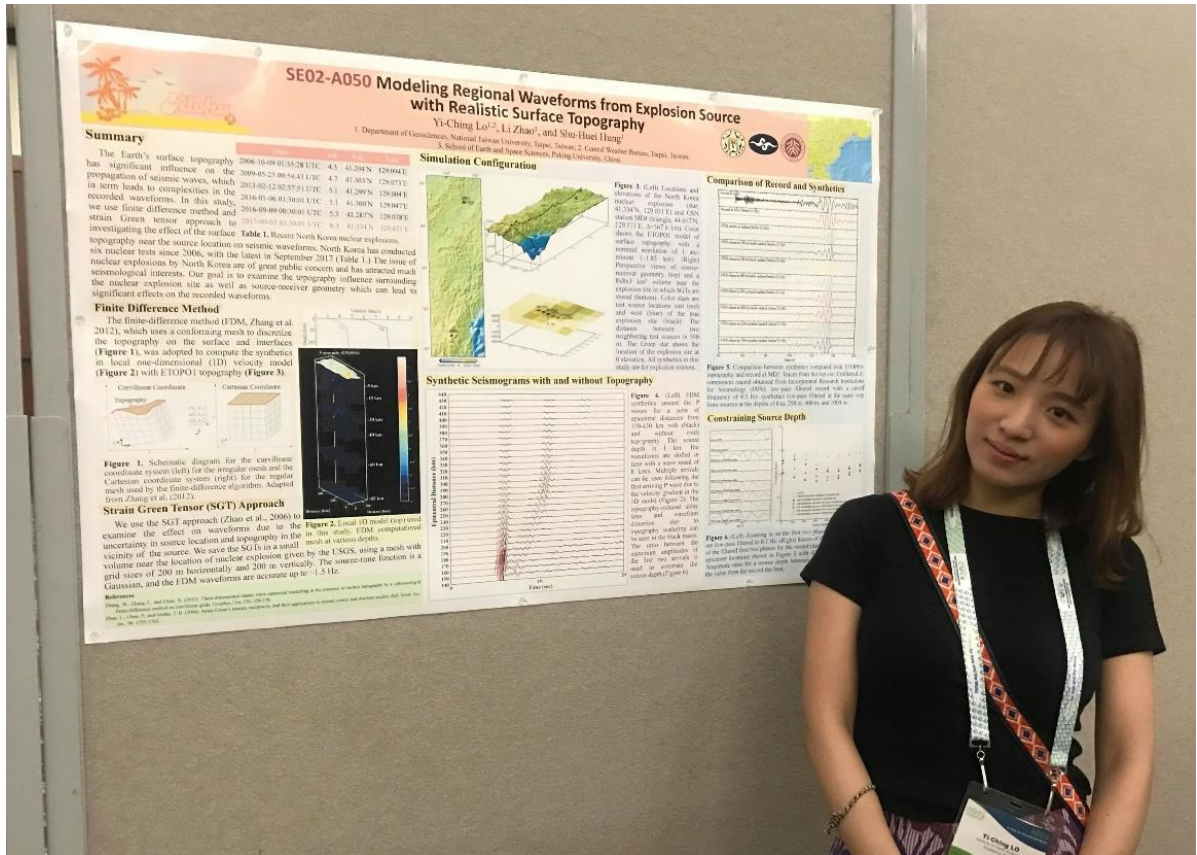
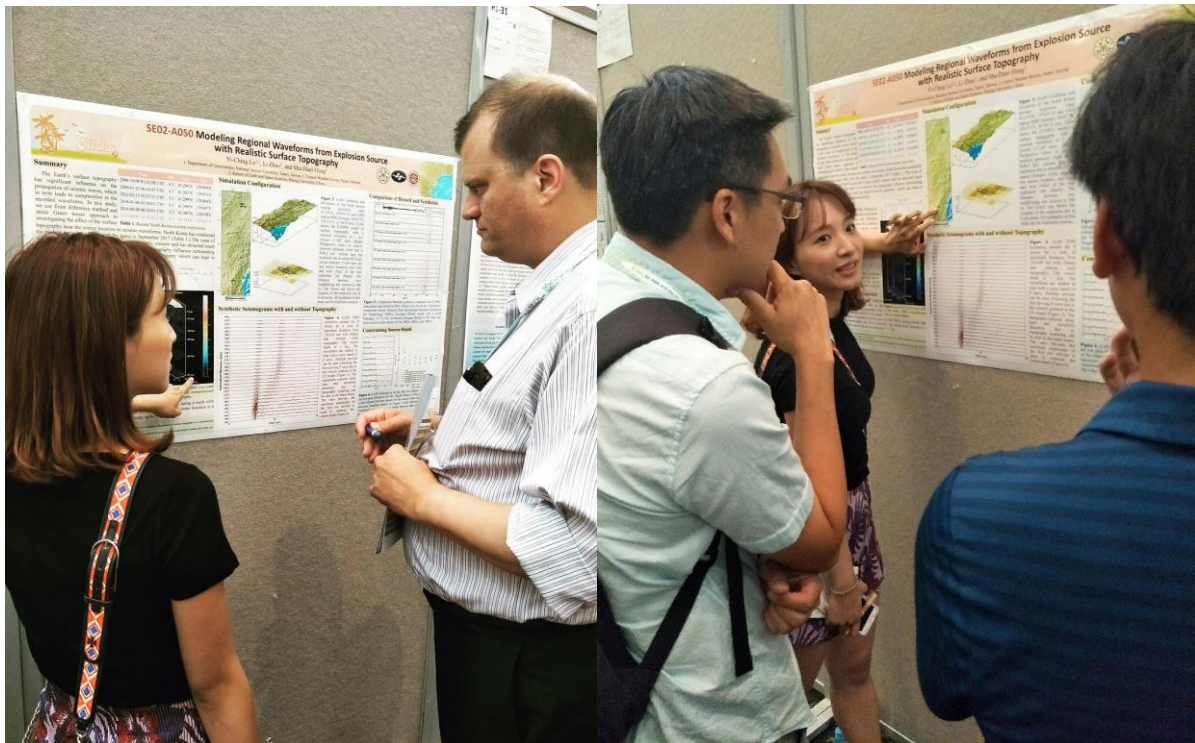


Figure 6. (Left) Zooming in on the first two phases. All waveforms are low-pass filtered to 0.3 Hz. (Right) Ratios of the peak amplitudes of the filtered first two phases for the record (dashed line) and for the 6 epicenter locations shown in Figure 3 with different source depths. Amplitude ratio for a source depth between 800 m and 1000 m fits the value from the record the best.

圖十、羅員發表之海報內容。



圖十一、羅員與海報合影。



圖十二、羅員與專家學者討論熱烈。

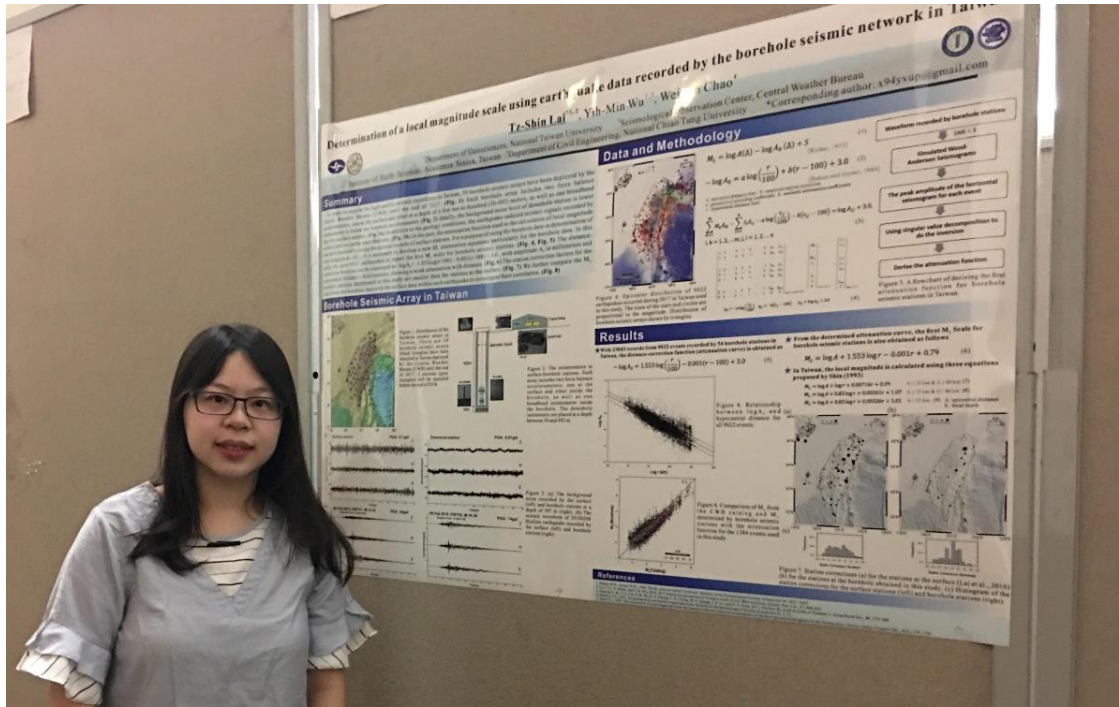
### 3. 賴姿心技佐：

賴員發表論文的題目為「Determination of a local magnitude scale using earthquake data recorded by the borehole seismic network in Taiwan」，研究內容為中央氣象局為了降低地表雜訊以獲得高品質地震訊號，至 2017 年底已建置 59 個井下地震儀陣列於全臺各地，每個陣列在地表及井下各有一部強震儀，井下另有一部寬頻地震儀，透過全臺井下地震儀陣列，提昇了小規模區域型地震的監測能力、地震定位的精準度及縮短強震預警的時間。

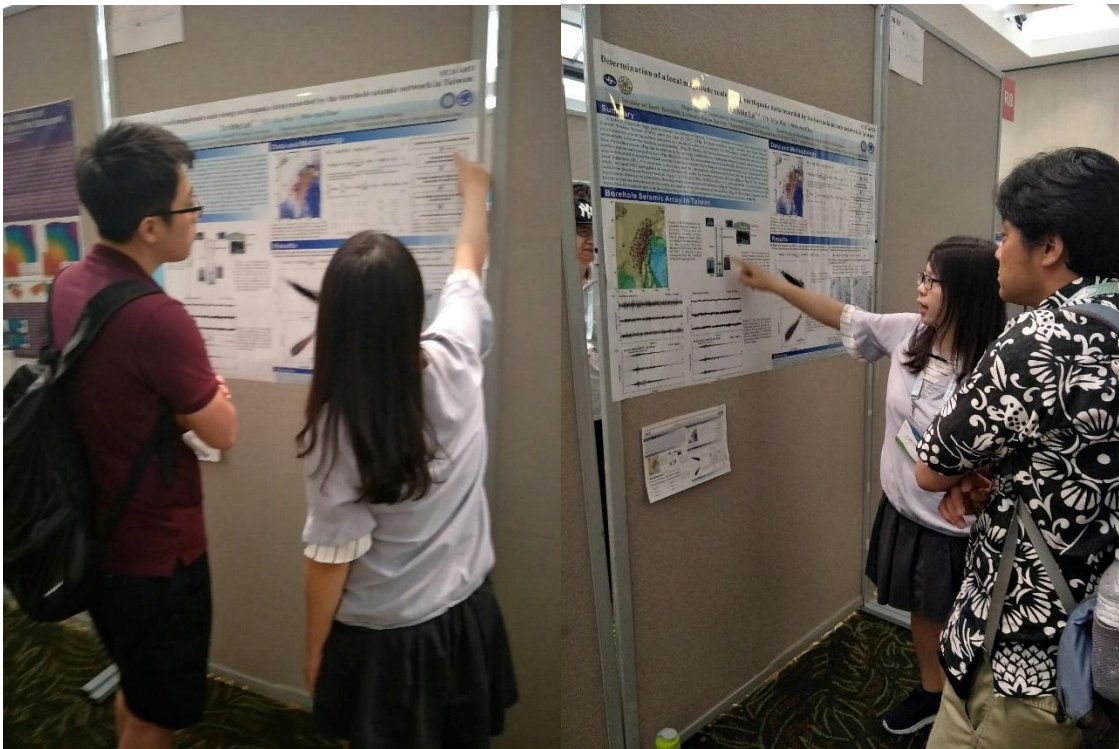
井下地震儀大多位於數百公尺深的岩盤上，雖然有效降低地表的雜訊，但對於地震訊號，由於場址地質條件的不同，井下站的加速度振幅會小於地表站，進一步造成地震規模的低估，而本局現有估算地震規模的測站皆為地表站，芮氏規模衰減式也是針對地表站，因此未來若要將井下地震儀資料納入地震規模使用，勢必要發展井下地震儀的芮氏規模衰減式，因此本研究使用臺灣井下地震儀資料，建立第一個針對井下地震儀的芮氏規模衰減式。







圖十四、賴員與海報合影。



圖十五、賴員與其他與會專家學者討論熱烈。

### 三、心得與建議

AOGS 每年都會換不同的地方舉辦會議，集結亞太地區的專家學者共襄盛舉，除了發表有關亞太地區地球科學的議題外，並提供與會學者深入討論及交流平台，今年的 AOGS 在夏威夷舉辦，開起會來既舒服又感受到當地濃濃的海島氣息。

亞洲及太平洋地區常發生許多天然災害，AOGS 每年辦理研討會就是希望各國專家學長能齊聚一堂針對各種災害性的議題進行成果發表或討論交流。

此次有此機會參加此一盛會，除了觀摩各國專家學者之成果，透由就近討論也給予與會人員許多研究上的建議。綜整心得與建議如下：

1. 本局地震測報中心在地震發生的第一時間，快速提供地震資訊供民眾與救災單位參用，其中地震規模的估算，因時效要求並未加入地震測站修正量，建議在後續資料處理時可以考慮納入地震測站修正量用以修正地震規模，提升地震芮氏規模的精準度。
2. 截至 2017 年底本局已於全臺各地建置 59 個井下地震儀陣列，然臺灣現行芮氏規模的估算僅使用地表測站，並未使用井下地震站之儀器資料，賴員已建立之 1 個井下地震儀的芮氏規模衰減式，未來應可持續研究，並評估將井下地震儀資料加入地震規模估算之可行性。另外，井下地震儀的資料極為珍貴，相關的應用與研究也可透過參與國際研討會發表成果，吸收其新知與經驗並應用於臺灣之發展。
3. 在速度構造逆推的方法上常用噪聲(Ambient noise)訊號去逆推淺層速度構造，此次議程上，已有學者使用結合體波逆推深層速度構造的研究，對速度模型的逆推在深度上有更完整的解析，提供未來了解臺灣複雜的造山運動構造一個新的思維。

#### 四、附錄-研討會相關照片



照片 1、攝於夏威夷國際會議中心(Hawaii Convention Center)前。



照片 2、大會報到現場及領取識別證。



照片 3、研討會現場與專家學者討論研究內容，圖左為現職新加坡南洋理工大學的 Sehngji Wei，圖右為現職北京大學的 Li Zhao



照片 4、會場內各地球科學領域之廠商展覽，圖為 google 的攤位。



照片 5、位於會場 Hawaii Convention Center 旁，每天從飯店走到會場必經過的 kahanamoku lagoon，是典型的海島國家。



照片 6、會議結束隔天正值夏威夷一年一度的泛太平洋節(Pan-Pacific Festival)，從我們飯店正好可以鳥瞰遊行隊伍。



照片 7、泛太平洋節(Pan-Pacific Festival)為期 3 天的年度盛事，有盛大的 Ho'olaule'a 封街派對、各式表演團體演出、草裙舞嘉年華，以及熱鬧歡騰的威基基大遊行。



照片 8、泛太平洋節(Pan-Pacific Festival)的 Ho'olaule'a 封街派對。